Mon. Not. R. Astron. Soc. **000**, 1–6 (1996) Printed 1 February 2008 (MN LATEX style file v1.4)

Discovering Galactic Planets by Gravitational Microlensing: Magnification Patterns and Light Curves

Joachim Wambsganss
Astrophysikalisches Institut Potsdam, An der Sternwarte 16, 14482 Potsdam, Germany; e-mail: jwambsganss@aip.de

Accepted 1996 August 9. Received 1996 June 10

ABSTRACT

The current searches for microlensing events towards the galactic bulge can be used to detect planetary companions around the lensing stars. The effect of such planets is a short-term modulation on the smooth microlensing lightcurve produced by the main lensing star. Current and planned experiments should be sensitive enough to discover planets ranging from Jupiter mass down to Earth mass. In order to be able to successfully detect planets this way, it is necessary to accurately and frequently monitor a microlensing event photometrically, once it has been "triggered".

Here we present a large variety of two-dimensional magnification distributions for systems consisting of an ordinary star and a planetary companion. We cover planet/star mass ratios from $m_{pl}/M_* = 10^{-5}$ to 10^{-3}. These limits correspond roughly to M_{Earth} and $M_{Jupiter}$, for a typical lens mass of $M_* \approx 0.3 M_\odot$. We explore a range of star-planet distances, with particular emphasis on the case of "resonant lensing", a situation in which the planet is located at or very near the Einstein ring of the lensing star.

We show a wide selection of light curves – one dimensional cuts through the magnification patterns – to illustrate the broad range of possible light curve perturbations caused by planets. The strongest effects are to be expected for caustic crossings. But even tracks passing outside the caustics can have considerable effects on the light curves. The easiest detectable (projected) distance range for the planets is between about 0.6 and 1.6 Einstein radii. Planets in this distance range produce caustics *inside* the Einstein ring of the star. For a lensing star with a mass of about $0.3 M_\odot$ at a distance of 6 kpc and a source at 8 kpc, this corresponds to physical distances between star and planet of about 1 to 3 AU.

Key words: gravitational lensing - dark matter - Stars: planetary systems

1 INTRODUCTION

The fraction of stars that have planetary companions is unknown. It is certainly not zero, and it can be as high as 100%. After the first discovery of a multiple planet system around pulsar PSR 1257+12 (Wolszczan & Frail 1992; Wolszczan 1994), recently various groups found "planets" around nearby stars, e.g. around Gliese 229A, 47 Ursae Majoris, 70 Virginis and 51 Pegasi (Mayor & Queloz 1995; Nakajima et al. 1995; Butler & Marcy 1996; Marcy & Butler 1996). These are reassuring observations, since it would have been bizarre if the sun would be the only star with a planetary system, and we lived in such a "special" place.

In the last few years, various groups have detected microlensing events caused by foreground objects passing in front of stars in the Large Magellanic Cloud or in the bulge of our Galaxy (Alcock et al. 1993; Udalski et al. 1993; Alard et al. 1995; Alard 1996). The idea goes back to Paczyński (1986) who suggested to use the gravitational lens effect of foreground objects on background stars for the search of dark matter in compact form in the Galactic Halo and Disk. By now more than 100 such microlensing events are recorded with the bulk of the durations between 10 days and 100 days (cf. Paczyński 1996a,b).

Most of these microlensing events follow very nicely the smooth symmetric light curves, as predicted by Paczyński (1986) or Griest (1991). Meanwhile a couple of non-standard events have been observed as well. These are without any doubt microlensed stars, but the lightcurve deviates clearly from the ideal shape of an isolated lens acting on an isolated background point source. Examples of such "perturbations" are the effect of the parallax of the Earth due to its motion around the sun during the event (Alcock et al. 1995), or light curves caused by binary lenses (Udalski et al. 1994a;

Dominik & Hirshfeld 1994; Mao & Di Stefano 1995). This proofs not only that the experiments are working in principle, but also that they are excellently doing the non-trivial job of accurately and frequently monitoring millions of stars and filtering out the highly interesting fraction of about 10^{-7} light curves affected by microlensing. And most importantly for our purpose here, these experiments are able to find microlensed lightcurves that deviate from the simple lightcurve of an isolated point lens.

In this paper we will investigate the effects of planetary companions to a star that acts as a microlens. Various aspects of microlensing by planets have been explored in the past. Mao and Paczyński (1991) were the first to suggest that these microlensing searches can be used to detect extra-solar planets. Gould and Loeb (1992) quantitatively estimated the fraction of microlensed light curves that are affected by planets (of Jupiter and Saturn mass), and the typical durations of the planetary perturbations. Bolatto and Falco (1994) perform a more refined and realistic analysis of the probability of detecting planetary companions for mass ratios down to 10^{-3}. Very recently Bennett and Rhie (1996) include the effect of the finite size of the source and show and emphasize that the microlensing searches are able to detect planets down to the Earth mass. In a recent review, Paczyński (1996b) also investigates the odds for detecting earth mass planets with gravitational microlensing.

After rederiving some relevant numbers and orders of magnitude in Chapter 2, we briefly present the ray shooting method in Chapter 3, which we use to determine the magnification properties of a star-planet system. A large variety of maps of the microlensing magnification as a function of the source location, produced by various planet/star mass ratios and a range of planet-star distances are shown in Chapter 4. Many example light curves – one-dimensional cuts through these two-dimensional magnification distributions – are presented to illustrate the wide range of possible light curve perturbations. In Chapter 5 we summarize our results and conclude with a brief comparison between the various methods to discover planets.

2 A FEW RELEVANT NUMBERS

The natural length scale for microlensing is the Einstein ring radius

$$R_E = \sqrt{\frac{4GM}{c^2}\frac{(D_S - D_L)D_L}{D_S}} = \sqrt{\frac{4GM}{c^2} D_S (1-d)\, d} \qquad (1)$$

where M is the mass of the lensing star, D_L and D_S are the distances to the lens and to the source, respectively, $d = D_L/D_S$ is the distance ratio, and G and c are the gravitational constant and the velocity of light. Parametrized by mass and distances, the Einstein ring radius in the lens plane can be expressed as follows:

$$R_E = 8.1\ (M/M_\odot)^{0.5} (D_S/8kpc)^{0.5} ((1-d)\,d)^{0.5}\ AU \qquad (2)$$

$$= 1.21 \times 10^{14}\ (M/M_\odot)^{0.5} (D_S/8kpc)^{0.5} ((1-d)\,d)^{0.5}\ cm.$$

In the source plane the physical size increases by the ratio $D_S/D_L = d^{-1}$. The Einstein angle, i.e. R_E in angular units, is given as

$$\theta_E = R_E/D_L \qquad (3)$$

$$= 1.0\ (M/M_\odot)^{0.5} (D_L/8kpc)^{-0.5} (1-d)^{0.5}\ mas.$$

The microlensing magnification as a function of time is given as

$$\mu(t) = \frac{u(t)^2 + 2}{u(t)\sqrt{u(t)^2 + 4}}, \qquad (4)$$

where $u(t)$ is the projected distance between lens and source at time t (in units of the Einstein radius). For a typical transverse velocity of $v_\perp = 200 km/sec * v_{\perp,200}$, the time scale of a microlensing event produced by a star with mass M is given as

$$t_E = R_E/v_\perp \qquad (5)$$

$$= 69.9\ (M/M_\odot)^{0.5}\ (D_S/8kpc)^{0.5}\ ((1-d)\,d)^{0.5}\quad v_{\perp,200}^{-1}\quad days.$$

For comparison with the duration of the "perturbations" discussed below, it is worthwhile to point out that a time interval corresponding to 1% of the natural unit is

$$t_{1\%} = 0.01 \times t_E \approx 7.3 (M/M_\odot)^{0.5}\ hours$$

for the values of $v_\perp = 200 km/sec$ and $D_L = 6kpc$, $D_S = 8kpc$.

A stellar radius of $1R_\odot$ transforms into an angular source size of $\theta_S \approx 0.001\,\theta_E$ for a source distance of $D_S = 8kpc$ as used above. Such values show that it is justified to consider the finite extend of the sources (cf. Witt & Mao 1994; Witt 1995), rather than treating them as point sources. In the examples of the lightcurves below, we use angular source radii of $\theta_S = 0.001\,\theta_E$.

The mass of the Earth is about $3 \times 10^{-6} M_\odot$. Since most potential lensing stars are somewhat less massive than the sun, a mass ratio of $m_{pl}/M_* = 10^{-5}$ can be assumed to roughly correspond to an Earth type planet. Similarly, $m_{pl}/M_* = 10^{-4}$ and 10^{-3} are not too far from representing the masses of Uranus ($M_{Uranus} = 4.4 \times 10^{-5} M_\odot$) and Saturn ($M_{Saturn} = 2.9 \times 10^{-4} M_\odot$), relative to a low mass main sequence star. Jupiter's mass would correspond to an even higher mass ratio in that case ($M_{Jupiter} = 9.5 \times 10^{-4} M_\odot$)

3 THE METHOD

In order to determine a two-dimensional magnification map of the star-planet system in the source plane we use the inverse ray-shooting technique (cf. Schneider & Weiss 1986, Kayser, Refsdal & Stabell 1986; Wambsganss 1990; Wambsganss et al. 1990). We "shoot" light rays backwards from an observer through a lens plane that consists of a star with mass M_* and a planetary companion with mass $m_{pl}/M_* = 10^{-3}, 10^{-4}$ or 10^{-5}. The rays are collected in the source plane, and the density of the rays at a particular location in the source plane is directly proportional to the magnification at this point.

In order to obtain a lightcurve from such a two-dimensional pattern, one has to consider a star with a certain brightness profile serving as the "source", and – as a first approximation – assuming a straight track of the background star relative to the lens-observer system. In other words, a

light curve is a one-dimensional cut through such a magnification pattern, folded with a source profile of a background star.

Below, most of the magnification patterns and light curves are displayed as the differences between the case "star plus planet" and "star without planet". The advantage of this representation is a gain in dynamical range. And – after all – this is the way those galactic planets will be detected: as the differences of an observed light curve and a theoretical one by an isolated lens (Paczynski 1986, Griest 1991).

For the ray shooting, the planets are placed at various distances to the main star. In Figure 1 the lens plane geometry of the various scenarios is illustrated. The star is indicated with a 'star' symbol at the origin of the coordinate system, and the various positions of the planets investigated are marked with little crosses. The dashed line marks the Einstein radius. The top panel (Figure 1a) illustrates the cases explored in detail in Section 4.1 and Figures 2, 3 and 4 with eight planets at the following positions: $x_{pl}/R_E \approx 0.57, 0.65, 0.74, 0.86, 1.16, 1.34, 1.55, 1.77$. These eight planets are mapped simultaneously for illustrative purposes. The lens positions are chosen such that the caustics appear about equidistant in the source plane at $\theta/\theta_E = -1.2, -0.9, -0.6, -0.3, 0.3, 0.6, 0.9, 1.2$. The middle panel (Fig. 1b) shows four planets at positions $x_{pl}/R_E = 0.57, 0.86, 1.16$ and 1.77. They are investigated individually and in detail in section 4.2, and displayed in Figures 5, 6 and 7. The lowest panel (Fig. 1c) with planet positions very close to the Einstein ring radius illustrates the cases of "resonant lensing" looked at more closely in Figures 8, 9 and 10, and commented on in section 4.3. ("Resonant lensing" is equivalent to an isolated lens with an external shear equal to unity, which is not treatable analytically.)

4 RESULTS: MAGNIFICATION PATTERNS AND LIGHTCURVES

Below we will present the magnification distributions and light curves in three ways. The first is a combined view of eight planetary companions on the same scale as the stellar lensing, in order to see the relative importance and the qualitative properties (Section 4.1). In the second part the lensing effects for four different planet-star distances are explored individually in detail (Section 4.2), and in the last part, we investigate the case of "resonant lensing", with four planet positions very close to the Einstein ring (Section 4.3).

4.1 Qualitative Features: Eight Aligned Planets

In Figure 2 the lensing effects of planets at various distances to the main lensing star are shown on the scale of the star. The magnification pattern in the source plane indicates the magnification as a function of position: the darker the gray, the higher the magnification. The black circle marks the Einstein ring of the star. There are small perturbations visible that are caused by individual planets. For simplicity, we superposed the action of eight aligned planets at distances between $x_{pl} = 0.57R_E$ and $x_{pl} = 1.77R_E$, mapped simultaneously for qualitative purposes. The geometric arrangement of the planets can be seen in Figure 1a. These lens positions translate into a range of locations of the caustics in the source plane between -1.2 and +1.2 in normalized units. Figure 2a (left panel) corresponds to planet masses of $m_{pl}/M_* = 10^{-3}$, Figure 2b (right panel) to $m_{pl}/M_* = 10^{-4}$.

Most obvious is the changing appearance of the caustics depending on the lens-star distance: For very large values of x_{pl} (the rightmost perturbation in the magnification pattern) the planet caustic – an astroid with four cusps connected by four folds – is very small and far outside the Einstein radius. It is obvious that the planet causes additional magnification, the region at and around the caustic is darker than the environment. For $x_{pl} \approx 1.618R_E$ the caustic would be exactly on the Einstein ring (not displayed here), and it keeps growing in size with decreasing x_{pl}. For the planet with the second largest distance ($x_{pl} \approx 1.55R_E$) the caustics are already inside the Einstein ring at $\theta = 0.9\theta_E$; the next two planet positions ($x_{pl}/R_E \approx 1.34$ and 1.16) correspond to caustic positions $\theta = 0.6\theta_E$ and $0.3\theta_E$ For values of x_{pl} approaching R_E, the planet caustic merges with the caustic of the main star at the center (cf. section 4.3). For planet positions $x_{pl}/R_E < 1.0$, the caustics lie on the opposite side of the star, and the character of the caustics has changed: Now there are two triangular caustics with an area of "depression" in between. That means that for certain source positions the effect of an additional planet around a microlensing star can be a "de-magnification", compared to the case of the star without the planet. With still smaller distance planet-star, the two triangular caustics get smaller, their relative separation gets larger. The distance values are $x_{pl}/R_E \approx 0.86$, 0.74, 0.65 for the caustic locations $\theta = -0.3\theta_E$, $-0.6\theta_E$, $-0.9\theta_E$. At $x_{pl} \approx 0.618R_E$ the pair of caustics would be at the distance of the Einstein radius "on the other side" of the lens. The leftmost caustics displayed here at $\theta = -1.2\theta_E$ correspond to $x_{pl} \approx 0.57R_E$. For still smaller planet-star distances, approaching $x_{pl} \approx 0$, the locations of the caustics approach infinity. This shows that the star-planet distance range which is most likely to be detected as a perturbation of a microlensed lightcurve by a star is roughly $0.5R_E \leq x_{pl} \leq 2.0R_E$. This is the distance range for which the planet-star caustics are located inside or near the Einstein ring radius of the star. ⋆ With typical distances of $D_L = 6kpc$ and $D_S = 8kpc$, this translates into a physical range of (projected) planet distances from the main star of $0.96AU \leq x_{pl}\sqrt{M_*/0.3M_\odot} \leq 3.8AU$, very interesting indeed for expected planets.

The strip containing the caustics produced by the planets in Figure 2 is displayed in Figure 3 in higher resolution and subtracted by the magnification that would be produced by the "main" star alone. All the maps here and below are such "difference" magnification maps. A grey level darker than average indicates magnification relative to the case of an isolated star, brighter than average means demagnification relative to the case of a star without planet. Figure 3a indicates the case of $m_{pl} = 10^{-4}M_*$, Figure 3b that of $m_{pl} = 10^{-5}M_*$. Here the light deflection of all the eight

⋆ For planet distances much smaller than 0.5 R_E or much larger than 2.0 R_E, the lensing signature is unlikely to be detected as a perturbation of the lightcurve of a lensed star, but rather as an individual microlensing event, which will be more difficult in practice.

planets is considered at the same time. The horizontal lines mark the tracks along which light curves are determined.

In Figure 4 light curves are displayed that correspond to sources with radius $\theta_S = 1 * 10^{-3}\theta_E$ and which move (relative motion compared to the planet star system!) along the tracks marked with lines in Figure 3. For comparison, the solid line indicates the "unperturbed" lightcurve by an isolated star without planets. Note that these lightcurves are determined for all the eight planets simultaneously being at the given positions. It can be seen that the lightcurves are affected by more than one planet. (All other lightcurves displayed below are calculated for a single planet only.) The time scale is in units of t_E. Note that the features produced by the planets can have quite high amplitudes, their widths are a few percent of an Einstein radius, i.e. they can last from a few hours up to about a day or so, for the typical values of velocity and distances used in Chapter 2.

4.2 Quantitative Features: Inside and Outside the Einstein Ring

Subsequently we show in more detail and more quantitatively magnification patterns and light curves. In Figure 5 the magnification effects for planets at distances of $x_{pl}/R_E \approx 0.57, 0.86, 1.16$ and 1.77 (cf. Figure 1b), resulting in positions of caustics in source plane: $\theta/\theta_E = -1.2$, -0.3, 0.3, 1.2, are shown separately, from left to right. The three rows show the magnification patterns for three mass values: $m_{pl}/M_* = 10^{-5}, 10^{-4}, 10^{-3}$ (from top to bottom).

Superimposed are contour lines that indicate differences in magnification relative to the case without a planet. The dashed line is the "average" magnification, dotted lines indicate demagnification relative to the case with no planet by $\Delta m = 0.05$ mag and 0.30 mag, solid contours indicate magnifications of Δm =-0.05 mag, -0.30 mag, -0.50 mag. Note the asymmetry of the contours.

Figure 6 shows the magnification patterns for these cases without the contours, but with 4 straight lines indicating the tracks along which lightcurves are determined and displayed in Figure 7. The three rows reflect the different mass ratios ($m_{pl}/M_* = 10^{-5}, 10^{-4}, 10^{-3}$ from top to bottom). The four columns correspond to the four values of planet-star distances mentioned above. We tried to avoid tracks parallel or perpendicular to the line planet-star, and also not to cross the caustic pattern "centrally", in order not to get an artificially large number of symmetric or high amplitude light curves.

In Figures 7 various "realistic" light curves are displayed for circular sources with radii $\theta_S = 1 * 10^{-3}\,\theta$ (again, the smooth, bell-shaped light curve which would be produced by the lensing star alone is subtracted, shown is the "difference light curve"). In Figure 7a examples for planet masses of $m_{pl}/M_* = 10^{-5}$ are shown. The four columns reflect the four different planet distances, and the four rows are the tracks 1 to 4. In Figure 7b (and 7c) the same is shown for $m_{pl}/M_* = 10^{-4}$ (and $m_{pl}/M_* = 10^{-3}$). What is very obvious is the large variety of light curves, shapes, durations, structures. The deviations range from very smooth to very peaky, from single bumps to multiple ups and downs. Nice symmetric, double peaked, M-shaped events are visible as well as highly asymmetric examples.

4.3 "Resonant Lensing": Planets Close to the Einstein Ring

Here we will explore in some detail the case of "resonant" lensing. This is a situation in which the planet is at or very close to the Einstein ring of the lensing star. Such a situation corresponds to the case of an isolated single lens with an external shear of $\gamma = 1.0$, a diverging case that is not easy to treat analytically. We place lenses at distances of $x_{pl}/R_E = 0.905, 0.951, 0.975, 1.025, 1.051, 1.105$ as illustrated in Figure 1c.

The resulting caustic patterns in the source plane are located at normalized distances of -0.20, -0.10, -0.05, +0.05, +0.10, +0.20. These non-linear combinations of the caustics of star plus planet appear quite bizarre and can create very unusually looking, often multi-peaked light curves. The amplitudes, though, are quite modest, so that resonant lensing is certainly not the most efficient way of detecting planets with lensing. In Figure 8a the magnification structures including the caustics are shown for the six cases mentioned above with $m_{pl} = 10^{-4}M_\odot$ (same in Fig.8b for $m_{pl} = 10^{-3}M_\odot$). As in Figures 5, we display "difference magnification maps" in the source plane, the magnification of the case star plus planet minus the magnification of the star alone. The coordinates are in Einstein radii in the source plane. The darker the color, the higher the magnification relative to the situation without planet. Note also the very bright and almost white regions, which indicate de-magnification relative to the case with no planets.

In Figure 9 there are lines superimposed on the magnification patterns for the case of "resonant lensing", indicating the tracks for which light curves are determined: left/right columns for $m_{pl}/M_* = 10^{-4}/10^{-5}$. The tracks were chosen not to be parallel to one of the axes, and not to purposely pass through a cusp point, which might result in a not representative very high magnification. The six rows represent the six different values for the planet positions (decreasing from top to bottom).

The light curves along these tracks are displayed in Figure 10. The four columns represent the four different tracks, the six rows reflect the different star-planet distances, as indicated. The case Figure 10a (10b) shows the light curves for the mass ratio $m_{pl}/M_* = 10^{-4}(10^{-3})$, for circular sources with radii $\theta_S = 10^{-3}\,\theta_E$.

The most remarkable thing about these light curves is the wealth of their structures. Ranging from little dips, small smooth peaks, with or without depression before the increase, to symmetric double peaks with depressed interior region, through asymmetric decrease-increase features to very complex multi-peak, multi-depression shapes, sometimes looking like two clearly separated structures. The duration of these noticable perturbations of the lightcurves of the lensing stars ranges from about one or two percent of the time unit t_E to a few dramatic cases which affect the lightcurve for a fraction of more than 15% t_E. This translates into durations from shorter than one day, to about a week at most, for the numbers used in Chapter 2.

5 SUMMARY AND CONCLUSION

Gravitational microlensing in the Galaxy provides the opportunity to detect planetary companions of stars. Planets

of Saturn mass (or higher) are comparably easily detectable, Uranus-type planets are certainly possible to detect as well, and even Earth-mass planets can be deteced in this way, if the photometry is accurate enough and densely enough sampled. We present here magnification maps produced by star plus planet systems for a variety of planet-star distances and planet-star mass ratios. These two-dimensional distributions show a wealth of caustic patterns of the planet-star system. We also present a variety of example light curves for finite sources, along tracks with various impact parameters and directions for all these cases. In particular we explore the case of "resonant lensing", where the planet is located very close to the Einstein ring radius of the main star. Such a configuration gives rise to particular interesting caustics (cf. Figs. 8a/b)

For a source radius of $\theta_S = 10^{-3}\,\theta_E$, (roughly a solar radius at a distance of a lensed star at 8kpc), we determine light curves, which show a very large range of complexity. The effect of planet lensing can produce peaks and dips in the smooth light curve of a single star alone, i.e. local magnification and de-magnification, relative to the case without planet. The perturbation/modulation of the smooth lightcurve by the planet can cause a large variety of structures. Amplitudes of a few percent for earth type planets and higher for more massive ones can be found for a fair fraction of the light curves that pass near the location of the caustic. The caustics of the planet fall inside the Einstein ring of the main star for star-planet separations of $0.618 \leq x_{pl}/R_E \leq 1.618$, which translates into physical distances of $1.19AU \leq x_{pl}(M_*/0.3M_\odot)^{0.5} \leq 3.2AU$, for lens (source) distances of 6kpc (8kpc). This is quite an interesting range for planet searches.

The duration of the planet-induced variations in the lightcurve of microlensed stars is often short, typically a few percent of the normalized time. In physical units this can range from about 10 hours to a few days at most. The current microlensing experiments (cf. introduction) do or try online data reduction so that events can be caught in real time and alarms can be triggered. There are at least two groups involved in immediate follow up programs of such alarms: PLANET collaboration – Probing Lensing Anomalies NETwork – (see Albrow et al. 1996), and GMAN – Global Microlensing Alert Network – (see Pratt et al. 1996). Early warning/alert systems (Udalski et al. 1994b; Pratt et al. 1996) and subsequent frequent and accurate photometry – all of which is in principle in place already – are the only requirements to make sure that sooner or later galactic planets down to earth mass will be found. It is imaginable that a "second alarm" can be issued, once the measured light curve starts to deviate from the predicted theoretical light curve, which carries the high probability of the detection of a small-mass companion. There are already plans to implement such planet searches by on a big scale (Tytler 1995, as cited by Witt & Mao 1996).

It appears that a search for earth mass (or more massive) planets by gravitational microlensing is a viable and certainly comparatively inexpensive way to discover planetary systems around other stars.. In principle it can be done with the current equipment, for higher efficiency it certainly helps if the groups involved get larger telescopes, which allow shorter and more frequent exposures, larger fields, which allows to monitor more stars, and more effective on-line data reduction and faster alarming, which increases the chance of good coverage of the candidate light curve.

Detecting planets by microlensing, which is explored here, can certainly not replace the other methods to detect planets, e.g. the "Doppler wobble" already successfully employed to find planets by Mayor & Queloz (1995), Marcy & Butler (1996) or Butler & Marcy (1996). It is a completely independent method, though, which will complement the methods used already. Searching for planets by microlensing has some strengths: it will be able to find star-planet-systems quite far away (up to many kiloparsecs), and probably can extend the mass range downward from Jupiter-type planets already with current technology. Detecting planets by microlensing has biases different from those of the other methods: Whereas the Doppler wobble technique is most sensitive to planets circling the main star very closely, and the astrometric attempts to find planets work best for planets very far out, microlensing can best detect planets in a relatively narrow (projected) distance range, corresponding to a few AU for typical lens-source and planet-star distances. This may possibly be of interest if one searches particularly for planets in a similar environment as the earth.

Once successfully found in large enough numbers, planets discovered by microlensing can be used extensively for statistical investigations of the kind: what fraction of stars with mass X has planets with mass Y or similarly. Such studies may ultimately help us understand the formation and evolution of our solar planetary system. A lot needs to be done theoretically, in order to provide the underlying groundwork for such tasks. A study naturally extending this one is in progress, in determining cross sections for detecting planets of different masses, at different distances from the star, and for sources of different sizes.

ACKNOWLEDGMENTS

It is a pleasure to thank Bohdan Paczyński for many valuable discussions at various stages of this project, and Peter Friedrich for his helpful advice on the production of the figures. I also like to gratefully acknowledge Kim Griest, Shude Mao, Stanton Peale, Jean Schneider and Hans-Jörg Witt for their careful reading of the manuscript and for providing me with many useful comments.

REFERENCES

Alard C., in: IAU Symposium 173, eds. C. S. Kochanek and J. Hewitt, p. 215 (1996)
Alard C., Mao S., Guibert J. , *Astron. Astrophys. Lett.* 300, L17 (1995)
Albrow M. et al., in: IAU Symposium 173, eds. C. S. Kochanek and J. Hewitt, p. 227 (1996)
Alcock C., Akerlof C.W., Allsman R.A., Axelrod T.S., Bennett D.P. et al., *Nature* 365, 621 (1993)
Alcock C., Allsman R.A., Alves D., Axelrod T.S., Bennett D.P., Cook K.H. et al., *ApJ* 454, L125 (1995)
Bennett D. P. & Rhie S. H., SISSA Preprint # 9603158 (1996)
Bolatto A.D. & Falco E.E., *ApJ* 436, 112 (1994)
Butler R.P. & Marcy G.W., *ApJ* 464, L153 (1996)
Dominik M. and Hirshfeld A.C., *A& A* 289, L31 (1994)
Griest K., *ApJ* 366, 412 (1991)
Gould A. & Loeb A., *ApJ* 396, 104 (1992)

Kayser R., Refsdal S., Stabell R., *A& A* 166, 36 (1986)
Mao S. & Di Stefano R., *ApJ* 440, 22 (1995)
Mao S. & Paczyński B., *ApJ* 374, L37 (1991)
Marcy G.W. & Butler R.P., *ApJ* 464, L147 (1996)
Mayor M. & Queloz D., *Nature* 378, 355 (1995)
Nakajima et al. *Nature* 378, 463 (1995)
Paczyński B., *ApJ* 304, 1 (1986)
Paczyński B., in: IAU Symposium 173, eds. C. S. Kochanek and J. Hewitt, p. 199 (1996a)
Paczyński B., *Ann. Rev. Astron. & Astrophys.* , 34, 419 (1996b)
Pratt M.R. et al., in: IAU Symposium 173, eds. C. S. Kochanek and J. Hewitt, p. 221 (1996)
Schneider P. & Weiss A., *A& A* 164, 237 (1986)
Tytler D., talk at Workshop on Extra-Solar Terrestrial Planet Detection (1995)
Udalski A., Szymański M., Kaluzny J., Kubiak M., Krzeminski W. et al., *Acta Astron.* **43**,289 (1993)
Udalski A., Szymański M., Mao S., Di Stefano R., Kaluzny J. et al., *ApJ* 436, L103 (1994a)
Udalski A., Szymański M., Kaluzny J., Kubiak M., Mateo M. et al., *Acta Astronomica* 44, 227 (1994b)
Wambsganss J., 1990 Ph.D. Thesis, Munich University; available as MPA report #550
Wambsganss J., Paczyǹski B., & Schneider P., 1990 *Astrophys. J.* **358**, L33
Witt H.J., *ApJ* 449, 42 (1995)
Witt H.J. & Mao S., *ApJ* 430, 505 (1994)
Witt H.J. and Mao S., in: IAU Symposium 173, eds. C. S. Kochanek and J. Hewitt, p. 233 (1996)
Wolszczan A. & Frail D.A., *Nature* 355, 145 (1992)
Wolszczan A., *Science* 264, 538 (1994)

FIGURE CAPTIONS

This paper has been produced using the Royal Astronomical Society/Blackwell Science LaTeX style file.

Figure 1. Geometry of the various star-planet configurations that are investigated below. The star symbol at the origin of the coordinate system marks the position of the "main" lensing star. The crosses indicate the positions of the planetary companions. The scale is in units of Einstein radii of the main lensing star. The dashed line shows the Einstein ring radius. a) Eight planets at distances between 0.57 and 1.77 R_E (investigated more closely in Figures 2, 3, 4); b) Four planets at positions $0.57R_E, 0.86R_E, 1.16R_E$ and $1.77R_E$ (explored individually in Figures 5, 6, and 7); c) Six planet positions close to the Einstein ring ("resonant lensing"): $x_{pl}/R_E \approx 0.905, 0.951, 0.975, 1.025, 1.051, 1.105$ (cf. Figures 8, 9 and 10).

Figure 2. Magnification distribution in the source plane for a star and (simultaneously) eight aligned planets at various distances to the star. The field ranges from -1.3 to +1.3 left to right and bottom to top (in units of Einstein radii). The positions of the planets along the x-axis are indicated in Figure 1a. The corresponding caustic features are located along the x-axis at positions $\theta_{caus}/\theta_E = -1.2, -0.9, -0.6, -0.3, +0.3, +0.6, +0.9, +1.2$ in the source plane (Note that the caustics for the planets which are inside the Einstein radius, but on the "right side" of the star, are projected to the "left side" in the source plane, due to the light deflection by the star). Magnification is displayed in gray color, darker gray means higher magnification. The gravitational lens action of the planets produces the features along the x-axis, four left of the position of the star (from the planets with their positions inside the Einstein ring) and four on the right hand side (from planets outside). Note that the planetary perturbations cause some regions to be magnified relative to the case without planets (darker than environment) as well as other regions to be demagnified (brighter). The black circle indicates the Einstein ring for the star alone. The left panel is for planet masses of $m_{pl} = 10^{-3}M_*$, i.e. an Saturn-type mass; the right panel is for $m_{pl} = 10^{-4}M_*$, rather a Uranus-like mass for a typical $M_* \approx 0.3M_\odot$.

Figure 3. Caustic regions from Figure 2 in higher resolution. What is shown here is a "difference magnification map" for a lens consisting of star plus eight planets: the magnification for lensing by an isolated star is subtracted, in order to get a higher dynamic range in magnification. Regions that are darker than the "average" gray are magnified relative to the case with no planet, those that are brighter are demagnified. a) The two panels correspond to the regions left and right of the origin for planet masses of $m_{pl} = 10^{-4}M_*$, respectively. b) same for $m_{pl} = 10^{-3}M_*$. Note the bright regions between the triangular caustics and directly outside the fold caustics: they represent positions that are demagnified relative to the case of lensing by a star alone. The thin black lines indicate the tracks for which light curves are displayed in Figure 4.

Figure 4. Lightcurves for the tracks indicated in Figures 3. a) planet masses $m_{pl} = 10^{-4}M_*$); b) planet masses $m_{pl} = 10^{-3}M_*$. The solid line is the light curve that would be obtained without a planetary companion. The dashed curves indicate the "top" track in Fig.3, the dotted curves indicate the "bottom" track. (Note that the left and right wings of the light curves may arise from different tracks.) The source is assumed to be a homogeneous disk with radius $\theta_S \approx 1 * 10^{-3}\theta_E$. The influence of planets on the lightcurve of a microlensed star can be upward and downward changes relative to the undisturbed case.

Figure 5. High resolution magnification patterns for various values of planet mass m_{pl} and planet-star distance x_{pl}. Shown is the magnification of the star-planet-system, minus the magnification of the star alone. The three rows correspond from top to bottom to planet masses of $m_{pl}/M_* = 10^{-5}$, 10^{-4}, and 10^{-3}. The four columns represent from left to right planet distances of $x_{pl} \approx 0.57R_E, 0.86R_E, 1.16R_E$ and $1.77R_E$ in the lens plane (cf. Figure 1b). This corresponds to positions of the centers of the caustics (in the source plane) of -1.2, -0.3, 0.3, 1.2. On top of the qualitative gray scale (darker means higher magnification), there are contour lines for more quantitative assessment: The dashed line means $\Delta m = 0.0 mag$, the solid lines indicate values higher than that of an isolated star: $\Delta m/mag = -0.05, -0.30, -0.50$, dotted contours mean demagnification relative to this case $\Delta m/mag = 0.05, 0.30$.

Figure 6. The same magnification patterns as shown in Figure 5, here with four straight lines indicating four different tracks along which light curves are determined. Rows from top to bottom correspond to planet masses $m_{pl}/M_* = 10^{-5}, 10^{-4}, 10^{-3}$, respectively. Columns from left to right represent planet-star distances $x_{pl}/R_E \approx 0.57, 0.86, 1.16$ and 1.77. All panels are the same size, 0.3 R_E at a side, centered at the positions of the caustics. The corresponding light curves are shown in Figure 7.

Figure 7. "Difference" light curves for circular sources with radii $\theta_S = 10^{-3}\theta_E$ along various tracks: a) For planet masses $m_{pl}/M_* = 10^{-5}$ (corresponding to the top row in Figure 6); The four columns reflect different planet-lens distances: $x_{pl}/R_E = 0.57, 0.86, 1.16$ and 1.77 (from left to right). The four rows correspond to the four tracks indicated in the respective magnification patterns in Figure 6. b) Same for $m_{pl}/M_* = 10^{-4}$, cf. middle row in Figure 6; c) Same for $m_{pl}/M_* = 10^{-3}$, cf. bottom row in Figure 6.

Figure 8. Magnification patterns for "resonant lensing", a star with a planetary companion of mass $m_{pl} = 10^{-4}M_*$ near the star's Einstein ring. Shown are six configurations for the lens positions indicated in Figure 1c. Displayed is the "difference magnification", i.e. the magnification of the system "star plus planet" minus the magnification of an "isolated star". Dark (bright) gray means magnification higher (lower) than with star alone. Coordinates are in Einstein radii of the star, with its position at the origin. b) Same for $m_{pl}/M_* = 10^{-3}$.

Figure 9. Magnification patterns as shown in Figure 8, with four straight lines indicating four different tracks along which light curves are determined. Rows from top to bottom: planet-star distance $x_{pl}/R_E \approx 0.905, 0.951, 0.975, 1.025, 1.051, 1.105$(cf. Figure 1c). Left column: planet mass $m_{pl}/M_* = 10^{-4}$. Right column: planet mass $m_{pl}/M_* = 10^{-3}$. All panels are the same size, 0.3 R_E by 0.15 R_E centered at the positions of the caustics. The corresponding light curves are shown in Figure 10.

Figure 10. a) Light curves for planet mass $m_{pl} = 10^{-4} M_*$ and planet positions near the Einstein ring radius (cf. Figures 1c), along the tracks indicated in Figure 9. The source sizes are $\theta_S = 10^{-3}\theta_E$. The six rows correspond to the six magnification patterns in Figure 9 with increasing distance of the planet (between $x_{pl}/R_E = 0.9$ and 1.1). The four columns represent the four tracks. b) Same for planet mass $m_{pl}/M_* = 10^{-3}$.

Fig. 1

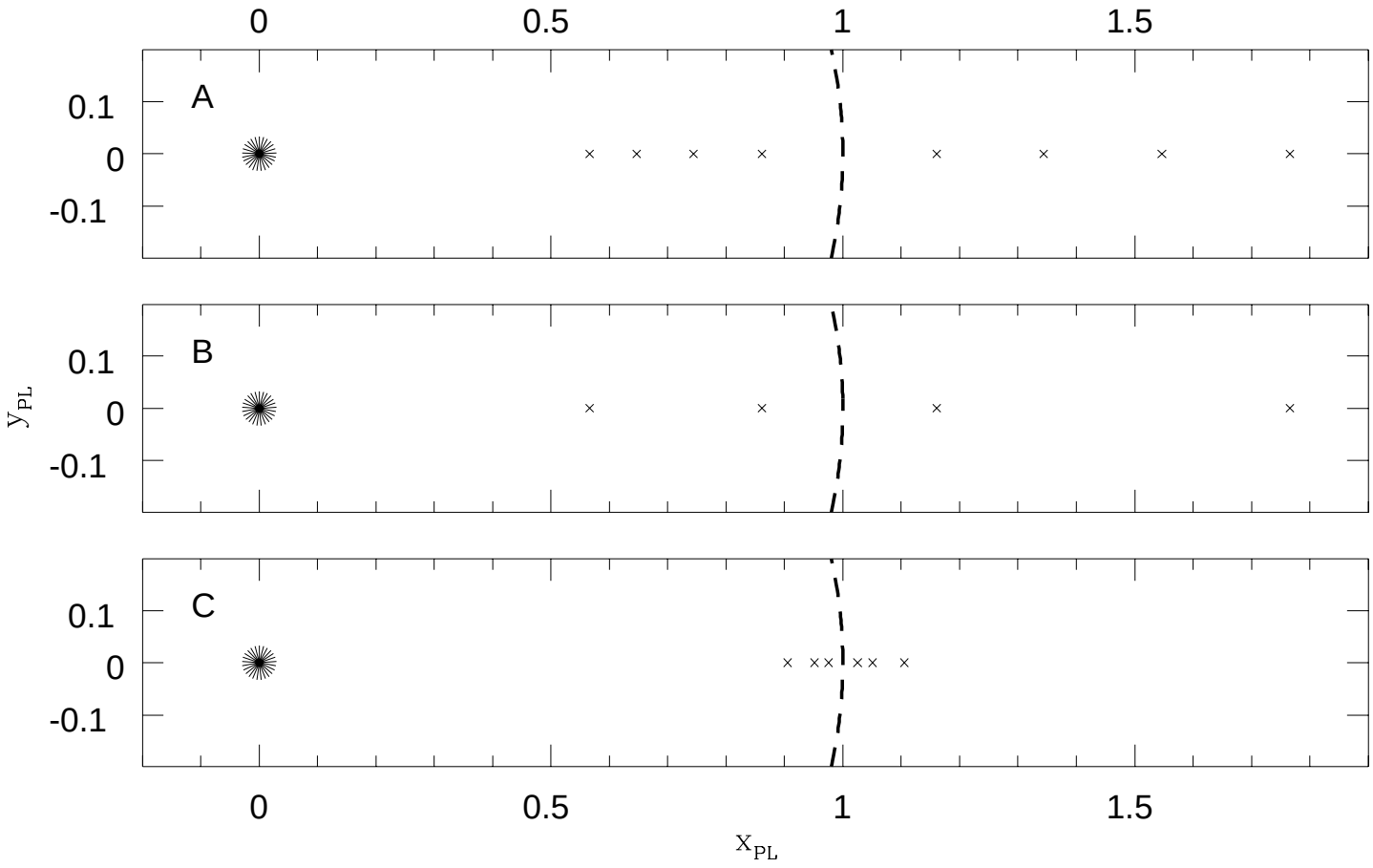

This figure "fig_2.jpg" is available in "jpg" format from:

http://arXiv.org/ps/astro-ph/9611134v1

This figure "fig_3a.jpg" is available in "jpg" format from:

http://arXiv.org/ps/astro-ph/9611134v1

This figure "fig_3b.jpg" is available in "jpg" format from:

http://arXiv.org/ps/astro-ph/9611134v1

This figure "fig_4a.gif" is available in "gif" format from:

http://arXiv.org/ps/astro-ph/9611134v1

This figure "fig_4b.gif" is available in "gif" format from:

http://arXiv.org/ps/astro-ph/9611134v1

This figure "fig_5.jpg" is available in "jpg" format from:

http://arXiv.org/ps/astro-ph/9611134v1

This figure "fig_6.jpg" is available in "jpg" format from:

http://arXiv.org/ps/astro-ph/9611134v1

This figure "fig_7a.gif" is available in "gif" format from:

http://arXiv.org/ps/astro-ph/9611134v1

This figure "fig_7b.gif" is available in "gif" format from:

http://arXiv.org/ps/astro-ph/9611134v1

This figure "fig_7c.gif" is available in "gif" format from:

http://arXiv.org/ps/astro-ph/9611134v1

This figure "fig_8a.jpg" is available in "jpg" format from:

http://arXiv.org/ps/astro-ph/9611134v1

This figure "fig_8b.jpg" is available in "jpg" format from:

http://arXiv.org/ps/astro-ph/9611134v1

This figure "fig_9.jpg" is available in "jpg" format from:

http://arXiv.org/ps/astro-ph/9611134v1

This figure "fig_10a.gif" is available in "gif" format from:

http://arXiv.org/ps/astro-ph/9611134v1

This figure "fig_10b.gif" is available in "gif" format from:

http://arXiv.org/ps/astro-ph/9611134v1